Chantal M. J. de Bakker
McKay Orthopaedic Research Laboratory,
Department of Orthopaedic Surgery,
Perelman School of Medicine,
University of Pennsylvania,
Philadelphia, PA 19104
e-mail: chantald@seas.upenn.edu

Wei-Ju Tseng
McKay Orthopaedic Research Laboratory,
Department of Orthopaedic Surgery,
Perelman School of Medicine,
University of Pennsylvania,
Philadelphia, PA 19104
e-mail: weits@pennmedicine.upenn.edu

Yihan Li
McKay Orthopaedic Research Laboratory,
Department of Orthopaedic Surgery,
Perelman School of Medicine,
University of Pennsylvania,
Philadelphia, PA 19104
e-mail: yihanl@seas.upenn.edu

Hongbo Zhao
McKay Orthopaedic Research Laboratory,
Department of Orthopaedic Surgery,
Perelman School of Medicine,
University of Pennsylvania,
Philadelphia, PA 19104;
Key Laboratory of Biorheological Science and
Technology,
Ministry of Education and Bioengineering
College,
Chongqing University,
Chongqing 400044, China
e-mail: zhhongbo@pennmedicine.upenn.edu

Allison R. Altman-Singles
McKay Orthopaedic Research Laboratory,
Department of Orthopaedic Surgery,
Perelman School of Medicine,
University of Pennsylvania,
Philadelphia, PA 19104;
Department of Kinesiology,
Pennsylvania State University,
Berks Campus,
Reading, PA 19610
e-mail: ara5093@psu.edu

Yonghoon Jeong
Division of Orthodontics,
College of Dentistry,
The Ohio State University,
Columbus, OH 43210
e-mail: yonghoonj@yahoo.com

Juhanna Robberts
McKay Orthopaedic Research Laboratory,
Department of Orthopaedic Surgery,
Perelman School of Medicine,
University of Pennsylvania,
Philadelphia, PA 19104
e-mail: robberts@seas.upenn.edu

Reproduction Differentially Affects Trabecular Bone Depending on Its Mechanical Versus Metabolic Role

During pregnancy and lactation, the maternal skeleton provides calcium for fetal/infant growth, resulting in substantial bone loss, which partially recovers after weaning. However, the amount of bone that is lost and the extent of post-weaning recovery are highly variable among different skeletal sites, and, despite persistent alterations in bone structure at some locations, reproductive history does not increase postmenopausal fracture risk. To explain this phenomenon, we hypothesized that the degree of reproductive bone loss/recovery at trabecular sites may vary depending on the extent to which the trabecular compartment is involved in the bone's load-bearing function. Using a rat model, we quantified the proportion of the load carried by the trabeculae, as well as the extent of reproductive bone loss and recovery, at two distinct skeletal sites: the tibia and lumbar vertebra. Both sites underwent significant bone loss during pregnancy and lactation, which was partially recovered post-weaning. However, the extent of the deterioration and the resumption of trabecular load-bearing capacity after weaning varied substantially. Tibial trabecular bone, which bore a low proportion of the total applied load, underwent dramatic and irreversible microstructural deterioration during reproduction. Meanwhile, vertebral trabecular bone bore a greater fraction of the load, underwent minimal deterioration in microarchitecture, and resumed its full load-bearing capacity after weaning. Because pregnancy and lactation are physiological processes, the distinctive responses to these natural events among different skeletal sites may help to elucidate the extent of the trabecular bone's structural versus metabolic functions.
[DOI: 10.1115/1.4038110]

Lin Han
School of Biomedical Engineering,
Science, and Health Systems,
Drexel University,
Philadelphia, PA 19104
e-mail: lh535@drexel.edu

Do-Gyoon Kim
Division of Orthodontics,
College of Dentistry,
The Ohio State University,
Columbus, OH 43210
e-mail: kim.2508@osu.edu

X. Sherry Liu[1]
McKay Orthopaedic Research Laboratory,
Perelman School of Medicine,
Department of Orthopaedic Surgery,
University of Pennsylvania,
426C Stemmler Hall,
36th Street and Hamilton Walk Philadelphia,
Philadelphia, PA 19104
e-mail: xiaoweil@pennmedicine.upenn.edu

Introduction

The skeleton has important mechanical as well as metabolic functions. In addition to bearing the loads applied during day-to-day living, the bones are also a reservoir for essential minerals, most notably calcium and phosphorus. During the physiological processes of pregnancy and lactation, the mother's skeleton forms an important source of calcium for fetal and infant growth, and as a result, these processes induce substantial maternal bone loss [1,2]. In clinical studies, women have been shown to undergo 5–7% decreases in bone mineral density as a result of lactation [3,4]. In rodent studies, bone loss is even more dramatic, as rats and mice show up to 30% reduction in bone mass by the end of lactation [5–7]. Although the maternal bone undergoes an anabolic period after weaning [8–10], the total extent of post-weaning recovery remains debated. Some argue that, because reproduction is not associated with increased risk of postmenopausal osteoporosis or fracture [2,11–17], the maternal skeleton must undergo a complete recovery following weaning, while others have shown that deficits in bone structure and/or mechanics remain long after lactation has ended [5,8,10,18–24]. Recent studies have also indicated that the extent of reproductive bone loss and recovery varies depending on the skeletal site that is assessed [5], and the trabecular regions, in particular, have been shown to recover incompletely after weaning [5,8,18,20,22,23].

Taken together, these findings that reproductive history does not adversely affect postmenopausal fracture risk, while inducing irreversible damage to specific trabecular bone sites, led us to hypothesize that the trabecular bone at skeletal sites that undergo irreversible bone loss during reproduction may play more of a metabolic, rather than a mechanical role. This would allow for permanent alterations in trabecular structure at such sites without increasing risk of fracture. Indeed, it has been shown that in rats, lactation bone loss results in preferential resorption of the central trabecular regions in the tibial metaphysis, as opposed to the trabeculae located in the medial and lateral metaphysis, which was hypothesized to be due to variations in the extent to which these different trabecular compartments participate in the tibia's load-bearing function [25]. Furthermore, a study in mice showed that while trabecular microstructure recovered fully after weaning at the spine, recovery was incomplete at the tibia and femur [5],

possibly due to differences in their relative roles in skeletal mechanics versus metabolism. Strikingly, female birds, which undergo a high demand for calcium during the egg laying period, are known to generate a specific type of metabolically active bone, termed "medullary bone" within the medullary cavities of certain long bones, which serves the purpose of providing a rapid source of calcium to allow for egg shell formation [26]. In contrast to cortical and trabecular bone, medullary bone is a rapidly formed woven bone that is often formed in isolated clusters and therefore plays a minimal role in bone mechanics [26]. Although the mammalian skeleton does not contain a distinct bone type that plays a solely metabolic role, it is likely that the trabecular bone in some regions of the skeleton, notably those that are surrounded by thick cortices that are able to bear the majority of the applied load, may have a similar function during times of high metabolic need such as reproduction. One such site which may play a largely metabolic role in the mammalian skeleton is the trabecular bone at the proximal tibia, as reproduction has been shown to induce dramatic, irreversible alterations in trabecular structure at this site with no long-term impact on whole-bone stiffness [27].

However, at other sites, trabecular bone does play a critical load-bearing function, and thus, permanent alterations in trabecular architecture would be expected to adversely affect fracture risk at these sites. One such site is the spine. In an ex vivo study of the human lumbar vertebra L3, trabecular bone volume fraction (BV/TV) was shown to be significantly correlated with the vertebral body failure load and stiffness with correlation coefficients (r) of 0.73 and 0.66, respectively, and the relationship between trabecular bone structure and whole-bone mechanics was even stronger when parameters of trabecular microarchitecture were included [28]. Studies evaluating the contributions of trabecular microstructure to vertebral mechanics in rats found similar results [29]. Furthermore, finite element (FE)-based evaluations of the distribution of load between the trabecular and cortical compartments in the spine have indicated that the vertebral trabecular bone is responsible for bearing approximately 40–80% of the applied load (depending on the location within the vertebral body) [30–32], suggesting that integrity of the trabecular microarchitecture is critical in maintaining the vertebra's load-bearing capacity.

Based on the relative extent of their roles in the skeleton's mechanical versus metabolic function, one might expect that

different trabecular sites will undergo distinct patterns of reproductive bone loss and recovery. In this study, we sought to explore the relationship between the fraction of the load applied to the trabecular bone and the reproduction-induced trabecular bone changes in a rat model. To do this, we quantified the trabecular load-share fraction and the extent of reproductive bone loss and recovery at two distinct skeletal sites: the tibia and vertebra. We hypothesized that the trabecular bone at the vertebra bears a larger fraction of the total applied load and thus plays a more critical role in the load-bearing function of that site. On the other hand, we expected that at the proximal tibia, the trabecular bone is less critical to the bone's load-bearing function, as it is surrounded by a thick cortical shell, thus allowing it to play a more metabolic role. Because of the crucial load-bearing function of the vertebral trabecular bone, we further anticipated that this site would undergo a lower degree of reproduction-induced structural deterioration and a larger degree of post-weaning recovery than trabecular bone at the tibia.

Methods

Animal Protocol. All animal experiments were approved by the University of Pennsylvania's Institutional Animal Care and Use Committee. Female, Sprague Dawley rats were assigned to four groups ($n = 6$/group): virgin, pregnancy, lactation, and 6-week post-weaning. Rats in the pregnancy group were mated, became pregnant, and were sacrificed at parturition. Rats in the lactation group underwent pregnancy as well as 2 weeks of lactation, and were sacrificed on lactation day 14. Rats in the 6-week post-weaning group also underwent pregnancy and lactation, were weaned on lactation day 21, and were allowed to recover for 6 weeks. To capture cell activities post-weaning, an additional group of rats was used (2-week post-weaning; $n = 6$), which were weaned on day 14 of lactation, and were allowed to recover for 2 weeks after weaning. To ensure sufficient dietary calcium content, rats were fed a high-calcium diet (LabDiet 5001 Rodent Diet; 0.95% Ca), as is the standard for rat studies of lactation bone loss [7,21,33]. All litters were normalized to nine pups per mother within 24 h of birth. One rat each in the lactation and 2-week post-weaning groups failed to become pregnant, resulting in a final sample size of $n = 5$ for the lactation and 2-week post-weaning groups, and $n = 6$ for all other groups.

All rats were sacrificed at age 6–7 months, and serum was collected immediately after sacrifice. The right tibiae and the first, second, and fourth lumbar vertebrae (L1, L2, and L4) were also dissected directly after sacrifice. L1 and L2 were stored in phosphate-buffered saline and frozen at $-20\,^{\circ}C$, and the right tibiae and L4 were stored in 70% ethanol.

Microcomputed Tomography Scans. On the day of sacrifice, all rats received in vivo microcomputed tomography (μCT) scans of the right proximal tibia, as described in Lan et al. [34]. Briefly, rats were anesthetized (4/2% isofluarane) and were fixed in a customized holder such that the right tibia was extended. A 4-mm long region of the tibia, located immediately distal to the proximal growth plate, was scanned at 10.5 μm resolution, with 145 μA current, 55 kVp energy, and 200 ms integration time, resulting in a total scan time of approximately 20 min.

To evaluate vertebral trabecular structure, L4 vertebrae were scanned ex vivo by μCT. Specifically, a 6 mm-long segment at the center of the vertebral body was scanned at 10.5 μm resolution, with 145 μA current, 55 kVp energy, and 300 ms integration time.

Finally, a 2 mm-long segment at the center of the L2 vertebral body was also scanned ex vivo at 20 μm resolution, with 145 μA current, 55 kVp energy, and 200 ms integration time, in order to estimate cross-sectional area for compression testing.

Microstructural Analysis. Trabecular bone microstructure was quantified at the proximal tibia and in the L4 vertebral body for all rats in the virgin, pregnancy, lactation, and 6-week post-weaning groups. At the proximal tibia, a 150-slice-thick trabecular volume of interest (VOI), located 2.5 mm distal to the growth plate, was isolated. At L4, a 200-slice-thick VOI was identified at the center of the vertebral body, located at the midpoint between the two endplates. All VOIs were manually defined so as to include all trabecular bone, and exclude the cortex. Within each VOI, bone tissue was isolated by applying a Gaussian filter (sigma = 1.2, support = 2), followed by a global threshold equal to 544 mg HA/cm^3. Finally, BV/TV, trabecular number (Tb.N), thickness (Tb.Th), and spacing (Tb.Sp), structure model index (SMI), and connectivity density (Conn.D) were evaluated [35].

Micro Finite Element Analysis. Whole-bone stiffness was computed for a 1.575-mm-thick region of the proximal tibia, located 2.5 mm distal to the growth plate, and for a 2.1-mm-thick region of the center of the L4 vertebral body for all rats in the virgin, pregnancy, lactation, and 6-week post-weaning groups, through microfinite element analysis. Each μCT image was downsampled by a factor of 1.5 to result in a final voxel size of 15.75 μm. To ensure consistent orientation, μCT images of the vertebra were aligned to a single template image through image registration (image registration was not needed at the tibia, as these scans were already highly aligned due to the use of the customized holder during in vivo μCT scans [34]). The tibia was then isolated from the fibula and the vertebral body was isolated from the processes, and images were Gaussian filtered (sigma = 1.2, support = 2), and thresholded (threshold equal to 544 mg HA/cm^3). Each bone voxel was converted to an eight-node brick element to construct the FE model, an axial displacement corresponding to 1% apparent strain was simulated, and the resulting reaction force was computed as described in Ref. [36]. Bone was modeled as a linear elastic material with Young's modulus of 15 GPa and Poisson's ratio of 0.3 [37].

Whole-bone stiffness was derived by dividing the reaction force by the total displacement. In addition, the fraction of the total load borne by the trabecular compartment was estimated at both sites. At both the tibia and vertebra, the distribution of load between the cortical and trabecular compartments varies substantially, depending on the location of analysis within the bone [31,38]. Therefore, to ensure consistency, the trabecular load-share fraction was computed at the same location within each site for each rat. The total reaction force and the reaction force exerted by the trabecular compartment at the proximal-most bone surface of the tibia image stack (located 2.5 mm distal to the proximal tibial growth plate) and at the caudal-most bone surface of the L4 image stack (located 1.05 mm caudal to the center of the vertebral body) were calculated (Fig. 3(a)). The trabecular load-share fraction was defined as the load supported by the trabecular bone, divided by the total load on the bone surface.

Static and Dynamic Bone Histomorphometry. All rats in the virgin, pregnancy, lactation, and 2-week post-weaning groups received subcutaneous injections of calcein (15 mg/kg, Sigma-Aldrich, St. Louis, MO) at 9 and 2 days prior to sacrifice, and the right tibiae and L4 were processed for undecalcified histology. Briefly, tibiae and L4 were stored in 70% ethanol prior to methyl methacrylate embedding. Methyl methacrylate-embedded samples were sectioned using a Polycut-S motorized microtome (Reichert, Heidelberg, Germany). For dynamic bone histomorphometry, 8 μm-thick sections were cut, and, based on the calcein labels, measurements of bone formation rate (BFR/BS), mineral apposition rate (MAR), and mineralizing surfaces (MS/BS) were made in the secondary spongiosa of the proximal tibia and at the center of the vertebral body in L4.

For static bone histomorphometry, 5 μm-thick sections were cut (Polycut-S motorized microtome, Reichert, Heidelberg, Germany). Sections were stained with Goldner's trichrome, and osteoblast number (Ob.N/BS), osteoclast number (Oc.N/BS),

osteoblast surface (Ob.S/BS), and osteoclast surface (Oc.S/BS) were measured at the same location where dynamic bone histomorphometry was performed. All static and dynamic histomorphometry measurements were made using Bioquant Osteo Software (Bioquant Image Analysis, Nashville, TN).

Serum Biochemistry Analysis. At sacrifice, blood was collected from all rats in the virgin, pregnancy, lactation, and 2-week post-weaning groups via cardiac puncture. Blood was maintained at room temperature for 30 min after collection to allow for coagulation, after which it was placed on ice and centrifuged at 200xg for 10 min to isolate serum. Serum levels of the resorption marker TRAcP 5b (TRAP) were measured (RatTRAP™ Assay, Immunodiagnostic Systems, Scottsdale, AZ).

Vertebral Compression Test. To further investigate the effects of reproduction on mechanical properties at a site that is largely made up of trabecular bone, L2 vertebrae from rats in the virgin, lactation, and 6-week post-weaning groups underwent compression tests. Vertebrae were dissected out, cleaned of soft tissue, and were scanned by μCT, as described earlier. The cranial and caudal ends of the vertebrae were cut using a low-speed diamond saw (Isomet, Buehler, Lake Bluff, IL) to produce parallel surfaces for uniaxial compression testing, following a procedure adapted from Pendleton et al. [39]. The processes were then removed, resulting in the isolation of a 4.04 mm-thick section of the vertebral body (corresponding to ~60% of the total vertebral body height), which was subsequently wrapped in saline-soaked gauze until testing.

After processing, the vertebral body was positioned between two parallel platens within the mechanical testing device (Instron 5542, Norwood, MA). Samples were compressed to failure at a displacement rate of 1.8 mm/min. Load-displacement curves were used to calculate peak load, stiffness, and energy to failure. Apparent-level properties, including ultimate stress, elastic modulus, and toughness, were estimated by normalizing extrinsic properties by μCT-derived total cross-sectional area, as described in Ref. [40].

Nanoindentation. L1 from rats in the virgin, lactation, and 6-week post-weaning groups were dissected free of soft tissue and were cut along the transverse plane using a low-speed diamond saw. The cut surfaces were polished using silicon carbide abrasive paper (with grit sizes of 1200, 2400, and 4000 grits), followed by Al_2O_3 paste (1 and 0.3 μm) in wet conditions. Finally, samples were sonicated in de-ionized water to remove debris, and were glued onto a holder mounted in the nanoindenter system (Nano-XP, MTS, Oak Ridge, TN), as described previously [41–43]. The trabecular bone was indented under wet conditions using a pyramidal Berkovich tip, at a displacement rate of 10 nm/second up to 500 nm indentation depth. After a 30-s holding period, bone was unloaded at 10 nm/s, and the slope of the unloading curve was used to compute the elastic modulus (E) based on the Oliver–Pharr method [44]. A total of 30 indents were performed for each sample, with 15 indents made on the surface regions of the trabeculae, and 15 indents made in the central regions of the trabeculae (Fig. 4(g)). Surface and center regions were identified using a light microscope contained within the nanoindenter system.

Statistical Analysis. All results are presented as mean±standard deviation. Differences among groups in trabecular microstructure, histological parameters, and bone mechanics were
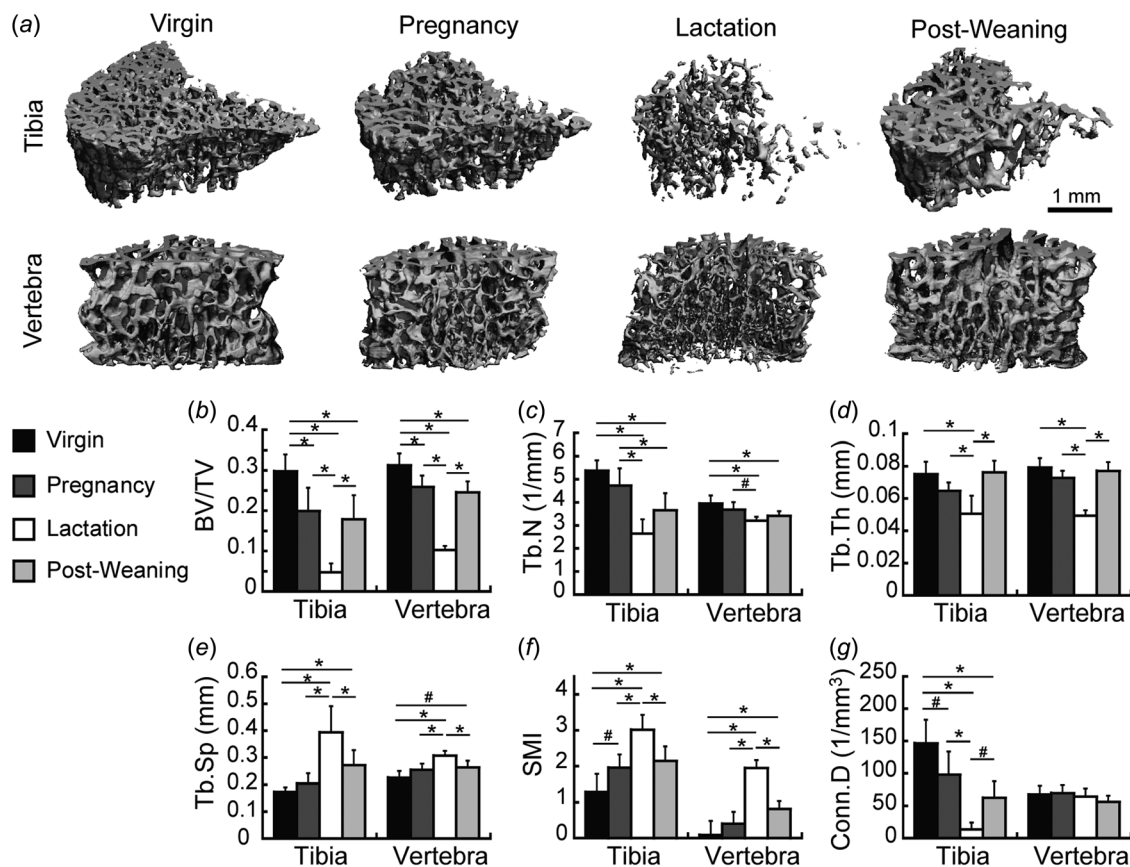

Fig. 1 (*a*) Representative three-dimensional renderings of trabecular microstructure at the proximal tibia and the L4 vertebra in virgin, pregnancy, lactation, and 6-week post-weaning rats. (*b*)–(*g*) Microstructural parameters at the tibia and L4 at each reproductive stage, including: (*b*) BV/TV, (*c*) Tb.N, (*d*) Tb.Th, (*e*) Tb.Sp, (*f*) SMI, and (*g*) Conn.D. * indicate significant differences among groups ($p < 0.05$), # indicate trends toward differences among groups ($p < 0.1$).

identified through a one-way analysis of variance. Upon the presence of statistically significant effects, post-hoc comparisons among groups were made using Bonferroni corrections. All analyses were performed using NCSS 7.1.4 (NCSS, LCC, Kaysville UT), and a two-tailed p-value below 0.05 was considered to indicate statistical significance.

Results

Site-Specific Changes in Trabecular Microarchitecture During Reproduction. At the proximal tibia, the trabecular microstructure was dramatically deteriorated as a result of reproduction (Fig. 1). At the end of pregnancy, BV/TV was 33% lower than in virgins. After 2 weeks of lactation, the microarchitecture was further deteriorated, with an 84% lower BV/TV compared to the virgin group. In addition, rats in the lactation group had reduced Tb.N, Tb.Th, and Conn.D, with elevated Tb.Sp and SMI, as compared to virgins. After weaning, there was a partial microstructural recovery, as the 6-week post-weaning group showed 274% greater BV/TV than the lactation group. However, the 6-week post-weaning group continued to have 40% lower BV/TV than virgins, and also had reduced Tb.N and Conn.D, and elevated Tb.Sp and SMI, indicating an incomplete recovery post-weaning.

At the lumbar vertebra, reproduction-associated changes in trabecular microstructure were generally similar to those observed at the proximal tibia. However, the degree of structural deterioration appeared to be less severe at this site (Fig. 1(a)). After pregnancy, rats had 17% reduced BV/TV compared to virgins, while lactation rats showed more substantial trabecular deterioration, with 67% lower BV/TV than virgins, in addition to reductions in Tb.N and Tb.Th and elevations in Tb.Sp and SMI. Trabecular microstructure at the L4 vertebra also underwent a period of post-weaning recovery, as indicated by the 140% greater BV/TV in 6-week post-weaning rats compared to the lactation group. Similar to the tibia, there were remaining deficits in trabecular bone structure at L4 post-weaning, as the 6-week post-weaning group showed 21% reduced BV/TV, along with a slight reduction in Tb.N and an elevated SMI, as compared to virgins. Overall, the degree of pregnancy- and lactation-associated trabecular deterioration, as well as the magnitude of the deficits in trabecular microstructure that remained at 6 weeks post-weaning, were substantially lower at the lumbar vertebra as compared to the proximal tibia. Notably, the vertebra showed no significant changes in Conn.D as a result of reproduction, and underwent a low degree of changes in Tb.N.
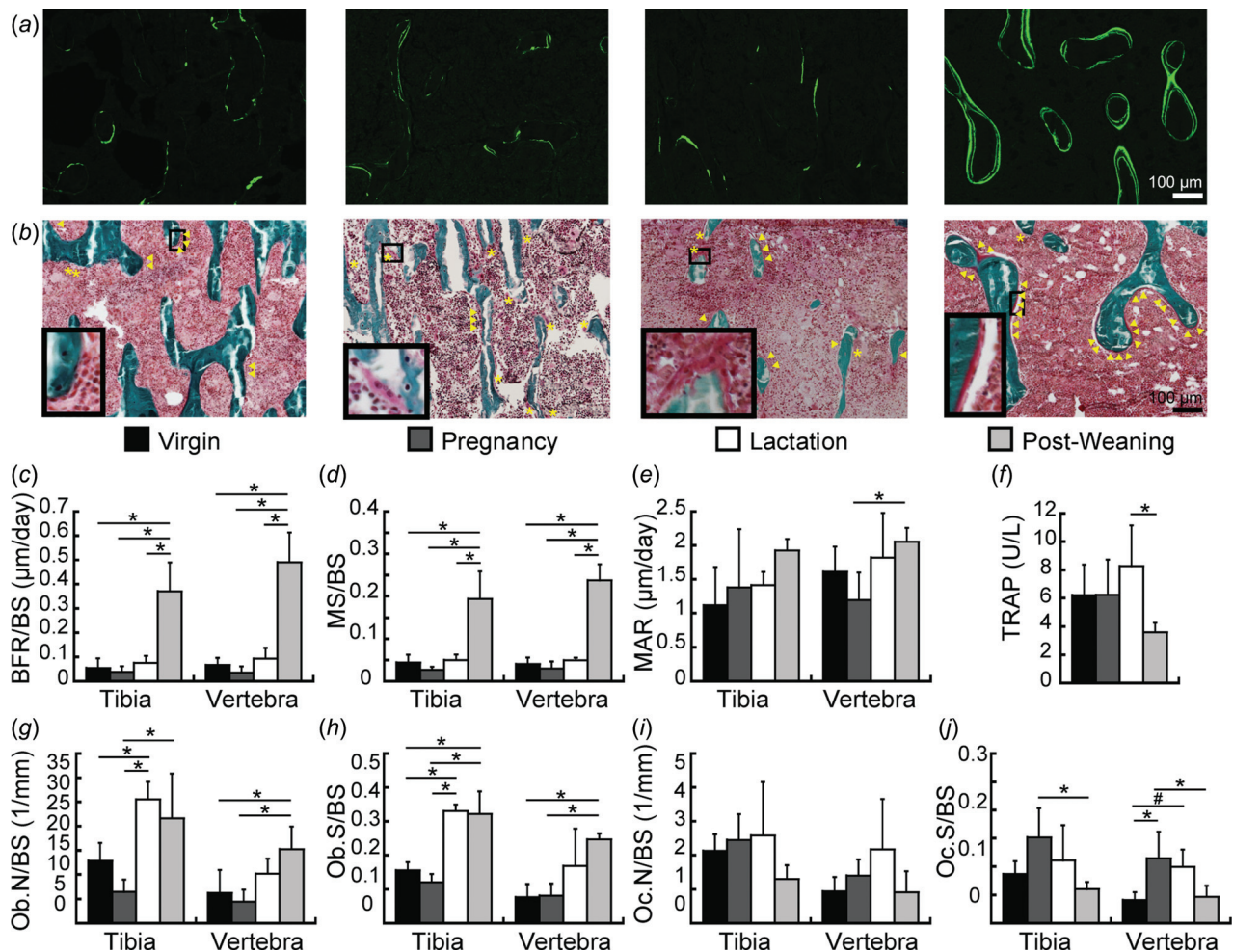
Fig. 2 Trabecular bone remodeling in virgin, pregnancy, lactation, and 2-week post-weaning rats. (a) Representative calcein-labeled histology slides used to evaluate bone formation. (b) Representative trichrome-stained slides. Triangles indicate osteoblast locations; asterisks indicate osteoclast locations. Close-up images of osteoblasts (in virgin and post-weaning groups) and osteoclasts (in pregnancy and lactation groups) are shown in the bottom left-corner of each slide. (c)–(e) Bone formation parameters during each reproductive phase, including (c) BFR/BS, (d) MS/BS, and (e) MAR, as quantified through fluorescent-labeled dynamic histomorphometry. (f) Serum TRAP. (g)–(j) Static histomorphometry-based cell numbers and surfaces, including (g) Ob.N/BS, (h) Ob.S/BS, (i) Oc.N/BS, and (e) Oc.S/BS. * indicate significant differences among groups ($p < 0.05$), # indicate trends toward differences among groups ($p < 0.1$).
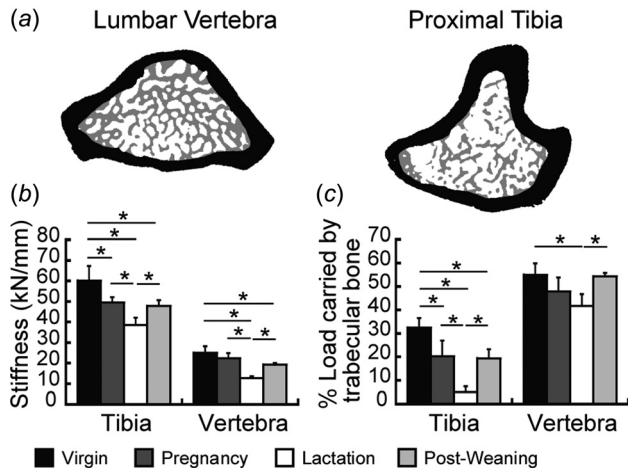
Fig. 3 Finite element analysis (FEA). (a) Schematic illustrating the isolation of trabecular (gray) and cortical (black) compartments at L4 (left) and the tibia (right) for calculation of load-share fraction. (b) Whole-bone stiffness and (c) trabecular load-share fraction in virgin, pregnancy, lactation, and 6-week post-weaning groups. * indicate significant differences among groups ($p < 0.05$).

Effects of Reproduction on Trabecular Bone Remodeling and Cell Activities. Static and dynamic histomorphometry and serum TRAP indicated minimal effects of pregnancy on bone remodeling or cell activities (Fig. 2). The only parameter that differed substantially between the pregnancy and virgin groups was Oc.S/BS, which was 178% elevated during pregnancy at the L4 vertebra. Similar to the pregnancy group, the lactation group also showed no differences from virgins in BFR/BS, MAR, MS/BS, Oc.N/BS, or serum TRAP. However, the lactation group did have 99% and 112% greater Ob.N/BS and Ob.S/BS than virgins at the tibia, with no differences in either parameter at L4. In addition, lactation rats showed a trend toward a 140% elevated Oc.S/BS compared to virgins at the vertebra ($p < 0.1$).

Following weaning, there was a systemic reduction in bone resorption, as indicated by 56% lower serum TRAP in the 2-week post-weaning group compared to the lactation group. In addition, the 2-week post-weaning group also showed 59–60% lower

Oc.S/BS than the pregnancy group at both the tibia and L4. Meanwhile, dynamic histomorphometry indicated rapid bone formation post-weaning, as the 2-week post-weaning group had 581% and 630% greater BFR/BS than virgins at the tibia and L4, respectively. This increase in bone formation appeared to result from an increase in mineralizing surface, as the 2-week post-weaning group also showed 337–485% greater MS/BS than virgins at both skeletal sites, while no differences were found between virgin and post-weaning rats in MAR. In addition, Ob.N/BS was 144% greater at L4 and Ob.S/BS was 107–221% elevated at both sites in the 2-week post-weaning group compared to virgins. Comparison of post-weaning indices of dynamic histomorphometry at the two sites by paired t-test indicated that the BFR/BS was 32% greater at L4 than at the tibia.

Site-Specific Effects of Reproduction on Whole-Bone Stiffness and Trabecular Load-Share Fraction. Microfinite element analysis indicated that whole-bone stiffness decreased as a result of reproduction at both skeletal sites (Fig. 3(b)). At the tibia, whole-bone stiffness was 18% lower in the pregnancy group and 36% lower in the lactation group than the virgin group. Although whole-bone stiffness increased 24% after weaning, 6-week post-weaning rats continued to show 20% lower whole-bone stiffness than virgins at the tibia. At the lumbar vertebra, there was no change in whole-bone stiffness associated with pregnancy; however, lactation rats had 49% lower whole-bone stiffness than virgins. Similar to the tibia, although there was a significant, 51% increase in vertebral stiffness after weaning, 6-week post-weaning rats continued to show 23% lower whole-bone stiffness than virgins.

Evaluation of the trabecular load-share fraction indicated substantial differences in the load distribution as well as in the patterns of reproductive bone loss/recovery, depending on the skeletal site (Fig. 3(c)). At the proximal tibia, virgin rats had a trabecular load-share fraction of 32%. Meanwhile, at L4, virgins had a trabecular load-share fraction of 55%, which was significantly greater than that at the tibia ($p < 0.0001$ by paired t-test), indicating that trabecular bone at the lumbar vertebra plays a larger relative role in load-bearing as compared to the proximal tibia. At the tibia, reproduction dramatically and irreversibly altered the load-bearing function of the trabecular bone: The tibial trabecular load-share fraction was 37% lower in the pregnancy group and 84% lower in the lactation group, as compared to virgin rats. Although
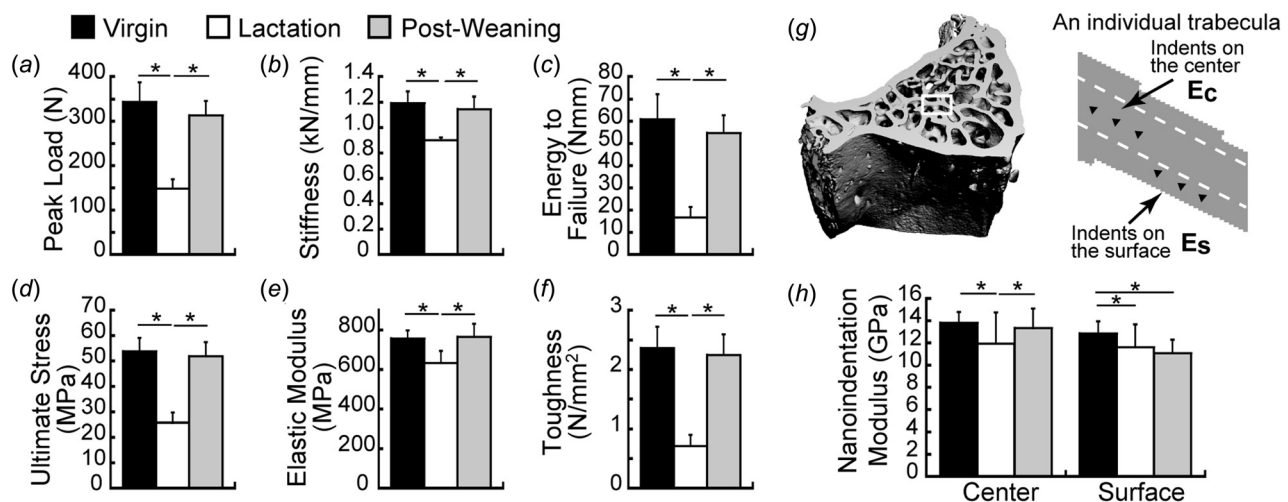
Fig. 4 Lumbar vertebra mechanics in virgin, lactation, and 6-week post-weaning rats. (a)–(c) Extrinsic properties of the vertebra measured through compression testing of L2: (a) peak load, (b) stiffness, (c) energy to failure. (d)–(f) Apparent-level properties derived through normalization of L2 compression results for bone size: (d) ultimate stress, (e) elastic modulus, (f) toughness. (g)–(h) Nanoindentation of L1: (g) schematic illustrating the locations where nanoindentation was performed to assess material properties of the surface and center regions of the trabeculae, (h) nanoindentation-based Young's modulus at the center and surface regions. * indicate significant differences among groups ($p < 0.05$).

the trabecular load-share fraction did recover significantly post-weaning, the 6-week post-weaning group continued to have 40% lower trabecular load-share fraction than virgins. At the lumbar vertebra, the trabecular load-share fraction underwent minimal changes as a result of reproduction. Rats in the lactation group showed 24% lower vertebral trabecular load-share fraction than virgins. However, by 6 weeks post-weaning, the vertebral trabecular load-share fraction had recovered fully.

Reproduction-Associated Changes in Vertebral Compressive Properties. To further evaluate the effects of structural changes on trabecular mechanics and bone tissue material properties, compression testing was performed at the L2 vertebra of rats in the virgin, lactation, and 6-week post-weaning groups. As shown in Fig. 4, reproduction induced deteriorations in whole-bone peak load, stiffness, and energy to failure, all of which were fully recovered after weaning. Similar trends were found when apparent-level properties were computed by normalizing whole-bone mechanics by vertebral size. Namely, lactation rats had reduced ultimate stress, elastic modulus, and toughness, as compared to virgins, while the apparent-level properties of 6-week post-weaning rats were not significantly different from those of virgins, indicating complete recovery of trabecular bone mechanics at the lumbar vertebra.

Reproduction-Induced Changes in Material Properties of Vertebral Trabecular Bone. Nanoindentation was performed on the trabecular bone of the L1 vertebrae of rats in the virgin, lactation, and 6-week post-weaning groups to more closely investigate the effects of reproduction on trabecular bone material properties. Indents were made at both the center and surface of the trabeculae (Fig. 4(g)), with variable patterns of reproduction-associated changes in nanoindentation modulus at these two locations. Lactation rats showed 10–14% reduced modulus at both sites, compared to virgins (Fig. 4(h)). After weaning, the central trabecular regions underwent a complete recovery. In contrast to this, the trabecular surface region continued to have a 14% reduced modulus in the 6-week post-weaning group, as compared to virgins.

Discussion

This study evaluated the effects of pregnancy, lactation, and weaning on trabecular bone microarchitecture, cell activities, and mechanics at two skeletal sites with distinct trabecular load-bearing roles: the proximal tibia and lumbar vertebra. Both sites showed similar general trends of reproductive bone loss and recovery, with a reduction in trabecular BV/TV during pregnancy and lactation, which was partially recovered post-weaning. However, the extent of the deterioration in trabecular microarchitecture and resumption of its load-bearing function after weaning differed substantially between the two locations. At the tibia, where trabecular bone was found to bear a low proportion of the total load applied to the bone, there was a dramatic deterioration of trabecular bone microarchitecture during pregnancy as well as lactation. In contrast to this, at the lumbar vertebra, where the trabecular bone bears a substantially greater share of the total applied load, there was minimal deterioration of the trabecular microarchitecture. Differences in the two skeletal sites continued post-weaning. Although both sites showed dramatically elevated bone formation activities after weaning, the post-weaning bone formation rate was significantly higher at the L4 vertebra than the proximal tibia. As a result, the trabecular bone at the vertebra resumed its full load-bearing function after weaning. In contrast, the tibial trabecular load-share fraction was not restored at the end of the post-weaning period. Because pregnancy and lactation are physiological processes, the differential trabecular response to these natural events at the lumbar vertebra versus the tibia may indicate differences in the extent of the trabecular bone's structural versus metabolic functions at these two locations.

Changes in trabecular bone microstructure during pregnancy, lactation, and post-weaning reported in this study were consistent with previous findings. At the rat proximal tibia, previous static histomorphometry-based and longitudinal, in vivo μCT-based evaluations also showed a high degree of pregnancy- and lactation-induced trabecular bone loss with microstructural deficits remaining up to three months post-weaning [8,27]. Previous studies evaluating the effects of reproduction on rat vertebral trabecular bone found a decrease in bone volume fraction (as measured through histomorphometry) associated with lactation, which underwent a period of recovery post-weaning [33]. Our findings of differential reproductive bone loss and recovery between the proximal tibia and lumbar vertebra are also in line with previous studies. Liu et al. evaluated changes in trabecular structure at the lumbar spine, proximal tibia, and distal femur in mice, and found that there was a substantial reduction in trabecular BV/TV as well as a deteriorated microarchitecture at all three sites at the end of lactation, but that only the lumbar spine had undergone a complete recovery by 28 days post-weaning [5]. Although this previous study did not quantify the trabecular load-share fraction at the three sites evaluated, the trabecular bone in both the mouse tibia and femur is surrounded by a dense cortex, which likely bears the majority of the applied load, suggesting that the trabecular bone at these sites may play a more metabolic role, similar to the current findings.

Quantification of cell activities and bone remodeling showed similar findings to those determined from μCT-based microstructural evaluations. In agreement with previous studies in both rats and mice [6,19,20,45], measurements of Oc.S/BS and serum TRAP suggested elevated osteoclast activity during the pregnancy and lactation periods, which dropped post-weaning. Calcein-labeled dynamic histomorphometry indicated an anabolic period post-weaning at both skeletal sites assessed, with dramatic elevations in bone formation rate as well as mineralizing surface at 2 weeks post-weaning, but minimal changes in mineral apposition rate. This finding is highly consistent with previous evaluations by Bowman et al. who also showed greatly increased rates of bone formation and mineralizing surfaces in the rat tibia after weaning, with a lower degree of changes in MAR [8]. Comparison of the parameters of bone formation between the two skeletal sites indicated a greater bone formation rate at L4 versus the tibia at 2 weeks post-weaning, possibly explaining the greater degree of post-weaning recovery at this site.

In addition to elevated rates of bone formation post-weaning, our findings also indicate elevated osteoblast number and surface during both the lactation and post-weaning periods. While post-weaning elevations in osteoblast numbers were expected, and agree with our μCT- and dynamic histomorphometry-based findings, the elevated osteoblast number and surface during lactation does not directly correlate with dynamic histomorphometry results. Previous studies measuring serum osteocalcin in mice also indicated similar trends, suggesting elevations in osteoblast numbers during lactation in addition to post-weaning [20]. Taken together, findings of elevated osteoblast as well as osteoclast activities during the lactation period are suggestive of a coupling between bone formation and resorption. A similar phenomenon has been found following menopause, where a net bone resorption occurs in the presence of elevated rates of both resorption and formation [46]. Interestingly, elevations in osteoblast numbers were not seen during pregnancy, in spite of similarly elevated rates of bone resorption during both the pregnancy and lactation periods. Thus, further investigation into the distinct bone remodeling mechanisms during these two reproductive phases is warranted.

In addition to the coupling of bone formation and resorption activities, the elevated osteoblast numbers observed during week 2 of lactation may also indicate a preparation of the bone tissue for the subsequent anabolic period post-weaning. Indeed, when evaluating the rat tibia at the end of 3 weeks of lactation, Bowman et al. found moderate elevations in bone formation rates, which further increased after weaning [8]. Further studies indicated high

rates of osteoblast proliferation and elevated bone formation immediately after weaning [9]. Because lactation and weaning are natural processes to which the skeletal physiology has been highly adapted, it is feasible that rates of osteoblast proliferation and osteoblast cell numbers may already begin to increase prior to weaning, in order to prepare for the upcoming anabolic period. Although the current study did not find an increased rate of bone formation (as measured through calcein labeling) at the end of the second week of lactation, the elevated osteoblast numbers observed at this time point may be an early indicator of subsequent post-weaning skeletal recovery. However, further investigation of the precise skeletal mechanisms governing the transition from lactation bone loss to the anabolic post-weaning period is critical to fully interpret these findings.

Evaluation of vertebral mechanics indicates that, in spite of the trabecular bone's metabolic role as a calcium source during reproduction, it undergoes a sufficient recovery post-weaning to maintain its structural role at sites where it plays a critical load-bearing function. In agreement with our findings, previous studies have also shown that, when tested in compression, the rat lumbar vertebra undergoes a deterioration in bone mechanics during lactation, with a decrease in peak load and stiffness, both of which are fully recovered after weaning [33]. In contrast to findings obtained from direct mechanical testing, our FE based evaluations of bone mechanics indicated a partial recovery of whole-bone stiffness post-weaning at both the tibia and L4: at both sites, FE-based whole-bone stiffness was found to be 20–23% lower than virgins at 6 weeks post-weaning. Discrepancies between results from direct mechanical testing (which showed a complete recovery of bone mechanics at the L2 vertebra after weaning) and FE-based evaluation of whole-bone stiffness may have arisen as a result of small differences between the vertebrae that were assessed through the two methods (FEA was performed at L4 whereas direct compression testing was performed at L2), or due to differences in the volume of interest within the vertebral body that was tested (due to limitations in the computational power of our FE model, FEA was performed on a region corresponding to the center 33% of the vertebral body, whereas direct compression testing was performed on the middle 60% of the vertebral body). Alternatively, differences in the extent of whole-bone stiffness recovery as measured through mechanical testing versus FEA may also be a result of assumptions of the FE model. The voxel-based FE model utilized in this study assumes constant and uniform bone tissue material properties, and therefore allows an accurate evaluation of the effects of trabecular and cortical bone microstructure on whole-bone stiffness. However, it is possible that reproduction may also have induced an improvement in bone material properties, which would allow for a full recovery of whole-bone mechanics in spite of continuing deficits in FE-derived whole-bone stiffness. Although post-weaning rats did not show an increase in modulus above virgin levels at the nanoscale, whole-bone mechanical properties arise as a result of bone properties at multiple length-scales. Thus, the discrepancy between the findings based on FEA and compression testing warrants further investigation into possible microscale adaptations occurring in the trabecular bone during reproduction.

Incomplete recovery in FE-derived whole-bone stiffness at the proximal tibia suggests a long-lasting, negative effect of reproduction on bone mechanics at this site. Several earlier reports have also noted incomplete recovery of bone mechanics after pregnancy and lactation at long-bone sites [5,33]. However, similar to the vertebra, FE-derived tibial stiffness also does not account for possible changes in tissue-level material properties. Thus, the possibility that improvements in bone material properties may have partially compensated for the deteriorated microarchitecture to preserve the mechanical function of the tibia cannot be excluded, and future mechanical testing will be required to confirm the effects of reproduction on mechanical properties at the tibia. Alternatively, the incomplete recovery of FE-derived tibial stiffness may also have been due to the timeframe of the study: similar

to the results reported here, our previous longitudinal in vivo μCT-based evaluation of bone changes at the proximal tibia also showed a reduced FEA-derived whole-bone stiffness at 6 weeks post-weaning after the first reproductive cycle [27]. Interestingly, this deficit was recovered after 3 sequential reproductive cycles, at which time the cortical bone at the proximal tibia was found to be more robust in post-weaning rats, while deficits in trabecular bone remained [27]. Taken together, results of the current study, where we found a dramatic and irreversible reduction in the trabecular load-share fraction at the proximal tibia as a result of reproduction, combined with our previous findings indicating subtle improvements of the cortical bone structure after reproduction [27], suggest that, at the tibia, the cortical bone may be able to compensate for reproduction-induced decreases in trabecular bone microstructure. However, although 6 weeks of recovery appears to be a sufficient time period to allow for post-weaning remodeling of the trabecular microstructure [8,27], our previous findings suggested that cortical bone adaptations may develop gradually over a longer time period [27]. As a result, the cortical bone remodeling process may have been incomplete at 6 weeks post-weaning, resulting in a reduced whole-bone stiffness.

This study also indicated interesting trends in bone tissue material properties as a result of reproduction. By performing nanoindentation at two distinct regions within the vertebral trabecular bone, reproduction-induced changes in bone tissue modulus were directly measured at both the surface and central regions of the trabeculae. At both sites, there was a decrease in modulus after lactation, indicating a reduction in bone tissue quality in addition to the structural deterioration observed through μCT. Previous studies have implicated the osteocyte perilacunar network as an important source of calcium during periods of high metabolic need such as lactation [47], which has been shown to significantly affect bone tissue quality [48]. Although direct quantification of the osteocyte lacunar/canalicular network was not performed in the current study, the reduction in bone tissue modulus at the central trabecular regions due to lactation and its recovery post-weaning are likely the result of the lactation-induced, reversible, osteocyte perilacunar/canalicular remodeling that has been previously reported [47,48]. Bone tissue modulus at the surface of the trabeculae was also found to be significantly decreased at the end of lactation. However, in contrast to the center of the trabeculae, the surface tissue modulus did not recover post-weaning. Our dynamic histomorphometry results indicate pervasive new bone formation on the trabecular surfaces following weaning. Thus, the persistently reduced modulus of the surface regions was likely due to incomplete mineralization of the newly formed bone tissue.

This study performs a robust comparison of the effects of pregnancy, lactation, and weaning on trabecular bone microstructure and mechanics at two distinct skeletal sites, which play variable roles in the skeleton's load-bearing and metabolic functions. However, this study has several limitations. Most notably, this was designed as a characteristic study, providing a reference for the differential effects of reproductive bone loss/recovery at different skeletal sites. Further studies will be required to investigate the mechanisms behind the varying patterns of reproduction-induced bone changes observed at the proximal tibia versus the lumbar vertebra. In addition, this study is limited in its use of the rat as an animal model. In particular, as a result of rats' quadrupedal motion, the lumbar vertebrae of the rat may not undergo the same loading patterns as the human lumbar spine. However, comparison of the trabecular load-share fractions measured here to clinical studies indicates a similar distribution of load between the trabecular and cortical compartments in both the rat and human spines [30–32]. Furthermore, by thoroughly evaluating the loading patterns in the quadruped spine, Smit demonstrated that, in spite of their positioning, the quadruped vertebrae are loaded axially as a result of the forces exerted by muscles and ligaments, with similar or possibly even higher magnitude forces than those applied to the human spine [49]. In addition, rodent models of lactation also differ from the clinical scenario in the source of the increased

calcium that is secreted during lactation: In humans, the calcium in milk is provided by skeletal resorption, regardless of the amount of calcium in the mother's diet [2]. However, because of their larger litter size and short duration of lactation, rodents rely on a combination of intestinal calcium uptake and skeletal resorption to provide the calcium needed during lactation [2]. Therefore, to maximize clinical applicability of this model and ensure sufficient dietary calcium content, the current study provided a high calcium diet containing 0.95% calcium.

Finally, the lactation and 2-week post-weaning groups in this study underwent 2 weeks of lactation, while the 6-week post-weaning group was allowed to lactate for a total of 3 weeks before being weaned. This may have resulted in greater deterioration of trabecular bone structure in the 6-week post-weaning group during its lactation phase. During the third week of lactation, however, rat pups begin to eat solid food, resulting in a decreased suckling intensity, and our previous longitudinal study in rats indicates a substantially reduced rate of trabecular bone loss at the proximal tibia after week 2 of lactation [27]; thus we do not expect the additional week of lactation in the 6-week post-weaning group to significantly impact the results reported here.

In summary, this study provided a thorough characterization of the effects of pregnancy, lactation, and weaning on trabecular microstructure and FEA-derived whole-bone stiffness at two distinct trabecular compartments. By evaluating changes in the proportion of the total load that is borne by the trabecular compartment at both the proximal tibia and lumbar vertebra, and correlating these changes to reproduction-induced changes in bone quality, this study provides important insight into the relative roles of the skeleton in providing mechanical support and in serving as a mineral reservoir to maintain homeostasis during periods of high metabolic demand. The differential effects of reproduction on trabecular bone sites with different relative roles in load-bearing, may in part explain the paradox that pregnancy and lactation result in dramatic maternal bone loss, which is incompletely recovered post-weaning, without adversely affecting postmenopausal fracture risk.

References

[1] Kovacs, C. S., 2011, "Calcium and Bone Metabolism Disorders During Pregnancy and Lactation," Endocrinol. Metab. Clin. North Am., **40**(4), pp. 795–826.
[2] Kovacs, C. S., 2016, "Maternal Mineral and Bone Metabolism During Pregnancy, Lactation, and Post-Weaning Recovery," Physiol. Rev., **96**(2), pp. 449–547.
[3] Kent, G. N., Price, R. I., Gutteridge, D. H., Allen, J. R., Barnes, M. P., Hickling, C. J., Retallack, R. W., Wilson, S. G., Devlin, R. D., Price, R. I., Smith, M., Bhagat, C. I., Davies, C., and St. Johns, A., 1990, "Human Lactation: Forearm Trabecular Bone Loss, Increased Bone Turnover, and Renal Conservation of Calcium and Inorganic Phosphate With Recovery of Bone Mass Following Weaning," J. Bone Miner. Res., **5**(4), pp. 361–369.
[4] Sowers, M., Corton, G., Shapiro, B., Jannausch, M. L., Crutchfield, M., Smith, M. L., Randolph, J. F., and Hollis, B., 1993, "Changes in Bone Density With Lactation," JAMA, **269**(24), pp. 3130–3135.
[5] Liu, X. S., Ardeshirpour, L., VanHouten, J. N., Shane, E., and Wysolmerski, J. J., 2012, "Site-Specific Changes in Bone Microarchitecture, Mineralization, and Stiffness During Lactation and After Weaning in Mice," J. Bone Miner. Res., **27**(4), pp. 865–875.
[6] VanHouten, J. N., and Wysolmerski, J. J., 2003, "Low Estrogen and High Parathyroid Hormone-Related Peptide Levels Contribute to Accelerated Bone Resorption and Bone Loss in Lactating Mice," Endocrinology, **144**(12), pp. 5521–5529.
[7] Zeni, S. N., Di Gregorio, S., and Mautalen, C., 1999, "Bone Mass Changes During Pregnancy and Lactation in the Rat," Bone, **25**(6), pp. 681–685.
[8] Bowman, B. M., Siska, C. C., and Miller, S. C., 2002, "Greatly Increased Cancellous Bone Formation With Rapid Improvements in Bone Structure in the Rat Maternal Skeleton After Lactation," J. Bone Miner. Res., **17**(11), pp. 1954–1960.
[9] Miller, S. C., Anderson, B. L., and Bowman, B. M., 2005, "Weaning Initiates a Rapid and Powerful Anabolic Phase in the Rat Maternal Skeleton," Biol. Reprod., **73**(1), pp. 156–162.
[10] Miller, S. C., and Bowman, B. M., 2004, "Rapid Improvements in Cortical Bone Dynamics and Structure After Lactation in Established Breeder Rats," Anat. Rec., Part A, **276**(2), pp. 143–149.
[11] Cummings, S. R., Nevitt, M. C., Browner, W. S., Stone, K., Fox, K. M., Ensrud, K. E., Cauley, J., Black, D., and Vogt, T. M., 1995, "Risk Factors for Hip Fracture in White Women. Study of Osteoporotic Fractures Research Group," N. Engl. J. Med., **332**(12), pp. 767–773.
[12] Cure-Cure, C., Cure-Ramirez, P., Teran, E., and Lopez-Jaramillo, P., 2002, "Bone-Mass Peak in Multiparity and Reduced Risk of Bone-Fractures in Menopause," Int. J. Gynaecol. Obstet., **76**(3), pp. 285–291.
[13] Hillier, T. A., Rizzo, J. H., Pedula, K. L., Stone, K. L., Cauley, J. A., Bauer, D. C., and Cummings, S. R., 2003, "Nulliparity and Fracture Risk in Older Women: The Study of Osteoporotic Fractures," J. Bone Miner. Res., **18**(5), pp. 893–899.
[14] Kauppi, M., Heliovaara, M., Impivaara, O., Knekt, P., and Jula, A., 2011, "Parity and Risk of Hip Fracture in Postmenopausal Women," Osteoporosis Int., **22**(6), pp. 1765–1771.
[15] Mori, T., Ishii, S., Greendale, G. A., Cauley, J. A., Ruppert, K., Crandall, C. J., and Karlamangla, A. S., 2015, "Parity, Lactation, Bone Strength, and 16-Year Fracture Risk in Adult Women: Findings From the Study of Women's Health Across the Nation (SWAN)," Bone, **73**, pp. 160–166.
[16] Petersen, H. C., Jeune, B., Vaupel, J. W., and Christensen, K., 2002, "Reproduction Life History and Hip Fractures," Ann. Epidemiol., **12**(4), pp. 257–263.
[17] Taylor, B. C., Schreiner, P. J., Stone, K. L., Fink, H. A., Cummings, S. R., Nevitt, M. C., Bowman, P. J., and Ensrud, K. E., 2004, "Long-Term Prediction of Incident Hip Fracture Risk in Elderly White Women: Study of Osteoporotic Fractures," J. Am. Geriatr. Soc., **52**(9), pp. 1479–1486.
[18] Affinito, P., Tommaselli, G. A., di Carlo, C., Guida, F., and Nappi, C., 1996, "Changes in Bone Mineral Density and Calcium Metabolism in Breastfeeding Women: A One Year Follow-up Study," J. Clin. Endocrinol. Metab., **81**(6), pp. 2314–2318.
[19] Ardeshirpour, L., Dann, P., Adams, D. J., Nelson, T., VanHouten, J., Horowitz, M. C., and Wysolmerski, J. J., 2007, "Weaning Triggers a Decrease in Receptor Activator of Nuclear Factor-KappaB Ligand Expression, Widespread Osteoclast Apoptosis, and Rapid Recovery of Bone Mass After Lactation in Mice," Endocrinology, **148**(8), pp. 3875–3886.
[20] Bornstein, S., Brown, S. A., Le, P. T., Wang, X., DeMambro, V., Horowitz, M. C., MacDougald, O., Baron, R., Lotinun, S., Karsenty, G., Wei, W., Ferron, M., Kovacs, C. S., Clemmons, D., Wan, Y., and Rosen, C. J., 2014, "FGF-21 and Skeletal Remodeling During and After Lactation in C57BL/6J Mice," Endocrinology, **155**(9), pp. 3516–3526.
[21] Bowman, B. M., and Miller, S. C., 1999, "Skeletal Mass, Chemistry, and Growth During and After Multiple Reproductive Cycles in the Rat," Bone, **25**(5), pp. 553–559.
[22] More, C., Bettembuk, P., Bhattoa, H. P., and Balogh, A., 2001, "The Effects of Pregnancy and Lactation on Bone Mineral Density," Osteoporosis Int., **12**(9), pp. 732–737.
[23] Bjornerem, A., Ghasem-Zadeh, A., Wang, X., Bui, M., Walker, S. P., Zebaze, R., and Seeman, E., 2016, "Irreversible Deterioration of Cortical and Trabecular Microstructure Associated With Breastfeeding," J. Bone Miner. Res., **32**(4), pp. 681–687.
[24] Brembeck, P., Lorentzon, M., Ohlsson, C., Winkvist, A., and Augustin, H., 2015, "Changes in Cortical Volumetric Bone Mineral Density and Thickness, and Trabecular Thickness in Lactating Women Postpartum," J. Clin. Endocrinol. Metab., **100**(2), pp. 535–543.
[25] Miller, S. C., and Bowman, B. M., 1998, "Comparison of Bone Loss During Normal Lactation With Estrogen Deficiency Osteopenia and Immobilization Osteopenia in the Rat," Anat. Rec., **251**(2), pp. 265–274.
[26] Whitehead, C. C., 2004, "Overview of Bone Biology in the Egg-Laying Hen," Poult. Sci., **83**(2), pp. 193–199.
[27] de Bakker, C. M., Altman-Singles, A. R., Li, Y., Tseng, W. J., Li, C., and Liu, X. S., 2017, "Adaptations in the Microarchitecture and Load Distribution of Maternal Cortical and Trabecular Bone in Response to Multiple Reproductive Cycles in Rats," J. Bone Miner. Res., **32**(5), pp. 1014–1026.
[28] Wegrzyn, J., Roux, J. P., Arlot, M. E., Boutroy, S., Vilayphiou, N., Guyen, O., Delmas, P. D., Chapurlat, R., and Bouxsein, M. L., 2010, "Role of Trabecular Microarchitecture and Its Heterogeneity Parameters in the Mechanical

Behavior of Ex Vivo Human L3 Vertebrae," J. Bone Miner. Res., **25**(11), pp. 2324–2331.

[29] Ito, M., Nishida, A., Koga, A., Ikeda, S., Shiraishi, A., Uetani, M., Hayashi, K., and Nakamura, T., 2002, "Contribution of Trabecular and Cortical Components to the Mechanical Properties of Bone and Their Regulating Parameters," Bone, **31**(3), pp. 351–358.

[30] Cao, K. D., Grimm, M. J., and Yang, K. H., 2001, "Load Sharing Within a Human Lumbar Vertebral Body Using the Finite Element Method," Spine (Philadelphia), **26**(12), pp. e253–e260.

[31] Eswaran, S. K., Gupta, A., Adams, M. F., and Keaveny, T. M., 2006, "Cortical and Trabecular Load Sharing in the Human Vertebral Body," J. Bone Miner. Res., **21**(2), pp. 307–314.

[32] Homminga, J., Weinans, H., Gowin, W., Felsenberg, D., and Huiskes, R., 2001, "Osteoporosis Changes the Amount of Vertebral Trabecular Bone at Risk of Fracture but Not the Vertebral Load Distribution," Spine (Philadelphia), **26**(14), pp. 1555–1561.

[33] Vajda, E. G., Bowman, B. M., and Miller, S. C., 2001, "Cancellous and Cortical Bone Mechanical Properties and Tissue Dynamics During Pregnancy, Lactation, and Postlactation in the Rat," Biol. Reprod., **65**(3), pp. 689–695.

[34] Lan, S., Luo, S., Huh, B. K., Chandra, A., Altman, A. R., Qin, L., and Liu, X. S., 2013, "3D Image Registration Is Critical to Ensure Accurate Detection of Longitudinal Changes in Trabecular Bone Density, Microstructure, and Stiffness Measurements in Rat Tibiae by In Vivo Microcomputed Tomography (muCT)," Bone, **56**(1), pp. 83–90.

[35] Bouxsein, M. L., Boyd, S. K., Christiansen, B. A., Guldberg, R. E., Jepsen, K. J., and Muller, R., 2010, "Guidelines for Assessment of Bone Microstructure in Rodents Using Micro-Computed Tomography," J. Bone Miner. Res., **25**(7), pp. 1468–1486.

[36] Hollister, S. J., Brennan, J. M., and Kikuchi, N., 1994, "A Homogenization Sampling Procedure for Calculating Trabecular Bone Effective Stiffness and Tissue Level Stress," J. Biomech., **27**(4), pp. 433–444.

[37] Guo, X. E., and Goldstein, S. A., 1997, "Is Trabecular Bone Tissue Different From Cortical Bone Tissue?," Forma, **12**, pp. 185–196.

[38] Little, R. B., Wevers, H. W., Siu, D., and Cooke, T. D., 1986, "A Three-Dimensional Finite Element Analysis of the Upper Tibia," ASME J. Biomech. Eng., **108**(2), pp. 111–119.

[39] Pendleton, M. M., Alwood, J. S., O'Connell, G. D., and Keaveny, T. M., 2016, "Design of Fatigue Test for Ex-Vivo Mouse Vertebra," Summer Biomechanics, Bioengineering, and Biotransport Conference (SB3C), Oxon Hill, MD, June 29–July 2, pp. 1115–1116.

[40] Hogan, H. A., Ruhmann, S. P., and Sampson, H. W., 2000, "The Mechanical Properties of Cancellous Bone in the Proximal Tibia of Ovariectomized Rats," J. Bone Miner. Res., **15**(2), pp. 284–292.

[41] Huja, S. S., Beck, F. M., and Thurman, D. T., 2006, "Indentation Properties of Young and Old Osteons," Calcif. Tissue Int., **78**(6), pp. 392–397.

[42] Kim, D. G., Huja, S. S., Lee, H. R., Tee, B. C., and Hueni, S., 2010, "Relationships of Viscosity With Contact Hardness and Modulus of Bone Matrix Measured by Nanoindentation," ASME J. Biomech. Eng., **132**(2), p. 024502

[43] Kim, D. G., Huja, S. S., Navalgund, A., D'Atri, A., Tee, B., Reeder, S., and Lee, H. R., 2013, "Effect of Estrogen Deficiency on Regional Variation of a Viscoelastic Tissue Property of Bone," J. Biomech., **46**(1), pp. 110–115.

[44] Oliver, W. C., and Pharr, G. M., 1992, "An Improved Technique for Determining Hardness and Elastic Modulus Using Load and Displacement Sensing Indentation Experiments," J. Mater. Res., **7**(6), pp. 1564–1583.

[45] Miller, S. C., and Bowman, B. M., 2007, "Rapid Inactivation and Apoptosis of Osteoclasts in the Maternal Skeleton During the Bone Remodeling Reversal at the End of Lactation," Anat. Rec., **290**(1), pp. 65–73.

[46] Kushida, K., Takahashi, M., Kawana, K., and Inoue, T., 1995, "Comparison of Markers for Bone Formation and Resorption in Premenopausal and Postmenopausal Subjects, and Osteoporosis Patients," J. Clin. Endocrinol. Metab., **80**(8), pp. 2447–2450.

[47] Qing, H., Ardeshirpour, L., Pajevic, P. D., Dusevich, V., Jahn, K., Kato, S., Wysolmerski, J., and Bonewald, L. F., 2012, "Demonstration of Osteocytic Perilacunar/Canalicular Remodeling in Mice During Lactation," J. Bone Miner. Res, **27**(5), pp. 1018–1029.

[48] Kaya, S., Basta-Pljakic, J., Seref-Ferlengez, Z., Majeska, R. J., Cardoso, L., Bromage, T. G., Zhang, Q., Flach, C. R., Mendelsohn, R., Yakar, S., Fritton, S. P., and Schaffler, M. B., 2017, "Lactation-Induced Changes in the Volume of Osteocyte Lacunar-Canalicular Space Alter Mechanical Properties in Cortical Bone Tissue," J. Bone Miner. Res., **32**(4), pp. 688–697.

[49] Smit, T. H., 2002, "The Use of a Quadruped as an In Vivo Model for the Study of the Spine—Biomechanical Considerations," Eur. Spine J., **11**(2), pp. 137–144.